

PACS 81.15.-z, 85.40.-e, 85.60.Jb

## **Si/A<sup>3</sup>B<sup>5</sup> one chip integration of white LED sources**

**Vladimir Osinsky<sup>1</sup>, Dmitry Murchenko<sup>1</sup>, Hooshmand Honarmand<sup>2</sup>**

<sup>1</sup>*Institute of Microdevices, Kyiv, Ukraine*

*E-mail: osinsky@imd.org.ua, espuntia@ukr.net*

<sup>2</sup>*Kyiv Polytechnic Institute, Kyiv, Ukraine*

*E-mail: hooshmand1980@yahoo.com*

**Abstract.** A<sup>3</sup>B<sup>5</sup> solid-state solution LEDs are highly desirable for their potential application in new emerging lighting technologies such as traffic signals, common lighting, architecture, signboards and communication. We present a solid-state integrated Si/A<sup>3</sup>B<sup>5</sup> device that consists of a single chip graded bandgap heterostructure with quantum well active layers, electron and hole injectors connected with Si MOS transistors integrated circuits. Active RGB layers are separated by tunnel barrier layers, which can be driven by transistors of the Si IC part of the chip. Ion stimulation of solubility of III-nitrides-arsenides and nano-template Al<sub>2</sub>O<sub>3</sub> epitaxy of GaN on Si substrate are presented. Self-organised nanostructures with a low dislocation density are obtained in this technology. Further optimization of epitaxy is likely to improve these results by at least an order of magnitude, drop the density of defects and increase luminescence quantum efficiency.

**Keywords:** RGB light mixing, A<sup>3</sup>B<sup>5</sup> compound, A<sup>3</sup>B<sup>5</sup> solid solution, quantum dot, epitaxy, solubility, solid-state lighting.

Manuscript received 20.03.09; accepted for publication 14.05.09; published online 15.05.09.

### **1. Introduction**

Hybrid and monolithic integration of solid-state lighting is needed in a wide variety of commercial and medical applications. In particular, integrated solid-state light sources represent a new class of optoelectronic devices, microprocessors and another scale integrated circuits (IC). Single chip solid-state lighting devices can actively and selectively route a large number of visual channels using only one light source, which provides significant advantages over existing devices. These advantages are in a simplified operating scheme, low driving currents, high switching speed, small size and low cost [1].

Si/A<sup>3</sup>B<sup>5</sup> white LED sources based on both multicomponent solid solutions and Si IC have not been investigated widely as caused by existing technological problems. Most of the commercially available LED lighting devices are made with traditional printed plate technology. In general, they have a great size and weight, and require relatively high driving currents ranging over a few kA, in contrast to their advantages of compability with silicon IC, ease of fabrication and low cost (Table).

In recent years, a large number of integrated Si/A<sup>3</sup>B<sup>5</sup> LED source technologies have been investigated [2]. However, a non-optimum energy efficiency, thermal problems and relatively high cost have raised significant

hurdles in the development of Si/A<sup>3</sup>B<sup>5</sup> LED source integration. In this paper, we report Si/A<sup>3</sup>B<sup>5</sup> white LED source technology based on hybrid and monolithic integration of RGB LEDs and Si IC. The fabricated Si/A<sup>3</sup>B<sup>5</sup> epitaxial structures use selective, lateral and template nanotechnology to give a small density of defects in the LED structures. It gives an increase in efficiency and low thermal heating of LED structures.

### **2. One chip RGB white LED concept**

In the widely known white LEDs, transformation of electric energy into optical radiation in the whole range of white light is inefficient as well as changes in time, which is predefined by the following factors:

- large concentration of defects in different heterostructures when cooling from the temperatures of epitaxy to the room one;
- concentration and range of sizes of quantum-well nanostructure is inadequate for the wide white spectrum of radiation;
- method of electron and hole injection in the known white LEDs does not provide even high-efficiency generation of radiation in the whole spectrum of white light;
- white light spectrum degradation in time.

**Table.** Characteristics of substrates for one chip white LED sources.

Substrate/Heterostructure property	Al <sub>2</sub> O <sub>3</sub>	SiC	GaN	AlN	GaN	GaAs	GaP	Si
Lattice parameter, Å	4.103	3.07	4.503		4.503-5.48	5.653	5.45	5.43
Thermal conductivity, W/cm·K	0.4	3.6	1.3	2.85		0.55	1.1	1.5
Thermal expansion match, 1/K	5.6·10 <sup>-6</sup>	3.8·10 <sup>-6</sup>	3.17·10 <sup>-6</sup>	5.3·10 <sup>-6</sup>		5.73·10 <sup>-6</sup>	4.65·10 <sup>-6</sup>	2.6·10 <sup>-6</sup>
Dislocation density, cm <sup>-2</sup>	10 <sup>9</sup>	10 <sup>5</sup>	10 <sup>4</sup>	10 <sup>4</sup>	10 <sup>8</sup>	10 <sup>3</sup>	10 <sup>3</sup>	<10 <sup>2</sup>
Substrate cost	M	H	H	M	H	M	M	L
Integration technology cost	H	H	H	H	M	M	M	L
White light transparency	H	H	H	H	M	L	M	L
Wafer diameter, inch	2	3	1	2	2	4	4	6

Note. M – middle, H – high, L – low.

In [3] the principle of a new superbright white LED based on heterogeneous semiconductor materials and structures is proposed.

This white superbright LED contains solid solution of A<sup>3</sup>B<sup>5</sup> (in particular AlGaInNAs) heterostructure of electron and hole injectors, active radiative layers formed from the metastable phases of multicomponent solid solutions (in particular AlGaInNPAsSb) and graded bandgap structure with quantum dots (Fig. 1a). The heterostructure of electron and hole injectors is created by a molecular beam or MOS-hydride epitaxy, and an active radiative layer is made by laser or ion-plasma stimulation of the growth process, next annealing and formation of the *p-n* junction that crosses all the thickness in the pitch of active layer area, thus a transition has a *p-n* junction of planar or another forms.

For best understanding the physical basis of this white LED, it is necessary to determine the mechanism of recombination in graded bandgap heterogeneous solid solution nitrides.

In binary compounds of AlN, GaN, InN and their solid solutions, a large role is played by defects, the most substantial of which are defects of lattice mismatch on the scopes of different atomic composition of layers. Minimization of defects plays a decisive role in obtaining the high efficiency and reliability of structures and devices in the wide spectrum of white LEDs.

To develop LED structures, it is necessary to use the methods of the bandgap engineering. In four, five, six, and seven component solid solutions of A<sup>3</sup>B<sup>5</sup>, there are areas where dissolution is absent. In these areas of the poor mixing, the heterogeneous solid solutions are created in micro- and nanoregions, and these are quantum structures [4].

In the systems of GaInN, GaNP, GaInNAs and AlGaInNAs, there are considerable areas of poor mixing at real temperatures of technological processes [5]. Calculations show that the critical temperature of a complete solution for these systems is a few thousand degrees. For example, for the GaNP system it is 7000 K. In traditional technologies aimed at preparation of

heterostructures, application of these temperatures is impossible. However, in nanoregions achievement of such high equivalent temperatures is possible by using local laser action or embodiment of ions into crystalline lattice. It extends the areas of solubility and removes the limit on preparation of any atomic combinations for the third and fifth groups of the periodic system, namely AlGaInNPAsSb.

For quarternary solid solution, the critical temperature (*T<sub>c</sub>*) is higher than for the three-component one; for the system GaInAsP *T<sub>c</sub>* = 1081 K, while for GaInP *T<sub>c</sub>* = 897 K.

From general statistical presentations, it is clear that growth in the number of different atoms increases the probability to obtain nanoclusters in macro- and micromatrixes of solid solutions. The sizes of nanoclusters at uncorrelated growth are possible to estimate from the statistically independent distribution of atoms in lattice [6].

For white LEDs, the offered basic system is a six- or seven-component system AlGaInNPAsSb with different correlations of components in the thickness of the heterostructure (Fig. 1a). In this multicomponent system *E<sub>g</sub>* changes from 6.2 eV for AlN down to 0.17 eV for InSb, which comprises all the visible range of wavelengths with fascination of ultraviolet and infra-red ranges at its ends. Binary compounds GaN and GaAs are basic in this structure [7]. Sapphire, silicon carbide, gallium arsenide, gallium phosphide or silicon can serve as substrates (Table).

For example, beginning the epitaxy growth of aluminum-gallium nitride structure on sapphire one passes to the system AlGaInN, where possible is considerable separation of phases at concentrations of In more than 12 %, and lattice mismatch for InN and GaN 11.3 %. Mismatch of AlN and InN lattices is higher 13.9 %. While mismatch of AlN and GaN lattices is only 2.3 %. Because of large mismatches in lattice parameters, the energy of internal strains even for well agreed lattice parameters of substrate and epitaxial layers accumulates in the system AlGaInN.

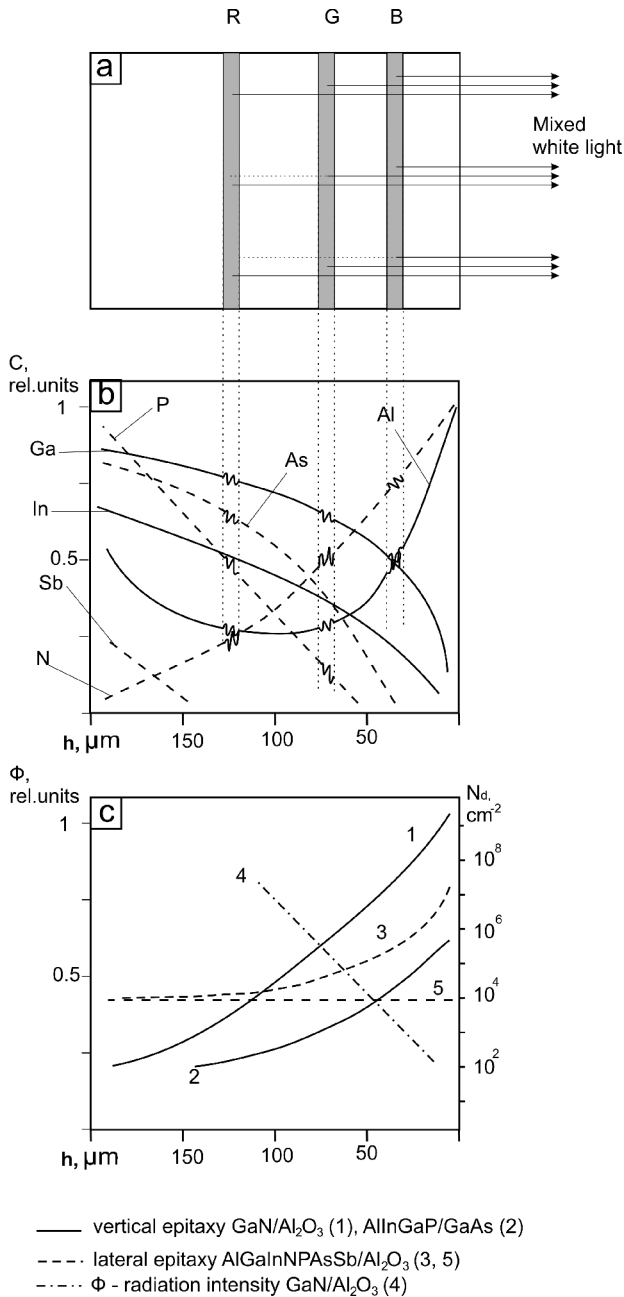


**Fig. 1.** (a) A schematic diagram of a three-color light mixing LED; (b) changes of solid solution components in AlGaInNPAsSb for single-chip white LED; (c) defect density  $N_d$  from structure thickness by vertical ion-stimulated epitaxy. 1 – GaN/Al<sub>2</sub>O<sub>3</sub>; 2 – AlInGaP/GaAs; 3 – lateral epitaxy AlGaInNPAs/Al<sub>2</sub>O<sub>3</sub>; 4 – luminescence intensity; 5 – defect density in substrate.

Epitaxial growth is carried out on sapphire substrates, starting from the layers of solid solutions that have a large width of the bandgap  $E_g$  with a gradual change of atomic composition, so that  $E_g$  is diminished adequately to decrease in quantum energy of radiation from blue to red of white spectrum scopes. Graded bandgap layers are consistently grown by alloying with donor impurities, without alloying and with alloying

with the acceptor ones. As a donor Si, Mg, Se or Te is used. As an acceptor Zn or Be is used. The active radiative layer is formed in such a manner that it contains metastable phases of solid solutions from which quantum wells and dots are formed using laser or ionic action with following annealing. They fill an active graded bandgap layer with a high density.

There are the following possibilities for monolithic integration of LED structures with silicon IC:

- epitaxial growth of A<sup>3</sup>B<sup>5</sup> structures on Si substrate,
- vertical selective epitaxy through “windows” in Si IC,
- lateral epitaxy on the surface of Si IC selective regions,
- vertical or lateral epitaxy on template layers on Si substrate.

In the case of vertical selective epitaxy, used is a nucleation plate made of sapphire, silicon carbide, zinc oxide or gallium nitride, on the surface of which a silicon integrating plate of 100 to 200  $\mu\text{m}$  thickness is fixed. In the process of chloride-hydride or ionic epitaxy with a high growth speed, holes are silted with gallium nitride and its solid solutions. After silting, the integrating substrate with silted selective areas is moved away from the base plate. Then, on the surface of selective areas, by the methods of molecular-beam epitaxy or the MOS-hydride one formed are multilayered heterostructures with the gradual change of atomic composition.

Growth from the ionized sources for the third and fifth groups of elements begins with gallium-aluminum nitride, gradually decreasing the concentration of aluminum and increasing the concentration of gallium, afterwards, ions and atoms of indium, arsenic and phosphorus are entered (Fig. 1a).

In Fig. 1b, the direction of atomic composition changes for aluminum, gallium, indium, nitrogen, phosphorus, arsenic and antimony are shown for this multilayered heterostructure.

Because heterostructures are formed from the ionized sources at the lowered temperatures, they do not have mechanical strains that appear when cooling after the epitaxial stage. Fig. 1c shows the surface concentration of defects that falls down to  $10^3$ - $10^2$   $\text{cm}^{-2}$  and is the lowest value for all-epitaxial structures [8, 9]. The intensity of recombination radiation here is several times increased, which provides a large efficiency of radiation in the visible range of spectrum. Gallium arsenide or phosphide can be used as a substrate. In this case, atomic composition of solid solutions in the layers of heterostructures changes in the direction of a gradual, layer-by-layer, increasing the width of the bandgap.

The amount and thickness of  $p$ - $n$  heterojunctions are determined by the descriptions of a specific white light source taking into account the technological parameters of preparing the multilayered structures by using computer facilities to control the processes of all-epitaxial growth and the microelectronic creation

processes for complex technological schemes. The technology to control composition developed in this work allows formation of a great number of LEDs and selective photodetectors in one chip. Thus, white light is synthesized from a great number of monochromatic spectra which are overlapped between each other.

The amount of radiative elements is equal  $N = \frac{\lambda_{\max} - \lambda_{\min}}{\Delta\lambda}$ , where  $\lambda_{\max} - \lambda_{\min}$  is the range of wavelengths representing white light,  $\Delta\lambda$  – middle linewidth monochromatic radiation at 2/3 of its height. Taking into account that the mean spectral width of light-emitting diode is 5 nm, for the dense filling of all the spectrum from 400 to 760 nm it is necessary to have 360 nm : 5 nm = 72 emitters. Real radiative subelements can be less or greater than this amount depending on the width of their monochromatic spectra and intensity of radiation. Selective photodetectors are chosen in such a manner that using Si microprocessor allow to control shortwave parts of the spectrum and support the parameters of sources in accordance with the chromaticity chart [11].

A white superbright light-emitting diode operates as follows. At the connection of the *p-n* junction to direct voltage, the injection of electrons and holes is realized in the space charge region where the quantum dots are located. Electrons and holes are injected into the quantum dots, where their recombination and emission of light quanta take place with the energy corresponding to the energy levels of electrons and holes. Since the recombination processes occur in all the layers of the graded bandgap structure, emitted are quanta of all the energy ranges in the forbidden band of this graded bandgap structure. It provides overlapping for the whole range of wavelengths in white light which goes out from the structure through the transparent substrate. Moreover, realized in quantum wells and dots is the wide spectrum of energy transitions predefined by different geometrical and energy parameters of quantum-sized structures, as well as by variations of the bandgap width related with mechanical strains in nanoregions. Thus, the wide white spectrum of radiation is provided simultaneously by three mechanisms that make the energy spectrum of transitions continuous and independent from different changes, for example, temperature. It stabilizes the spectrum of white superbright LED, which advantageously distinguishes them from the known technical solutions. Modern methods of planar technology of micro- and nanostructures allow to create a lot of planar *p-n* junctions with different topology in one chip, which provides optimization of the electric current value and radiation output in a LED structure. In particular, in the process of LED structure formation on an opaque substrate, such as Si or GaAs, multilayer mirrors are created on their surface for reflection of light, and the growth of a graded bandgap layer can begin with semiconductor material possessing a small bandgap.

Three individual LED chips or layers – red, green, blue (RGB) – can be combined to generate a mixing lighting and form a white light-emitting device. However, the production cost of such a hybrid LED is high, and the effect of thermal conductivity is not optimal, because the powerful individual chips should be mounted together for light mixing. It is possible to produce a white LED by using a single LED chip together with a yellow phosphor. However, endurance of the yellow phosphor is much shorter than that of the blue LED chip, thus limiting the lifetime of the white LED.

### **3. Light mixing control by quantum well barrier layers**

A light mixing white LED chip can be made from comprising multiple active layers with different energy bandgaps for emitting colored light with different wavelengths, to generate mixed light of a broad emission spectrum. In this case, the quantum well active layers have different energy bandgaps, and are separated by barrier layers having different energy bandgaps, too [10]. Also, the energy bandgap of a barrier layer adjacent to a *p*-type GaN side is smaller (or 20 % smaller) than that of a barrier layer adjacent to an *n*-type GaN side, while an energy bandgap of a quantum well layer adjacent to the *n*-type GaN side is larger than that of a quantum well layer adjacent to the *p*-type GaN side. In other words, the wavelength of light emitted from an active layer adjacent to the *n*-type GaN side is shorter than that from an active layer adjacent to the *p*-type GaN side, causing an overflow effect of conductive carriers, and resulting in coincidence luminescence from the quantum well layers. Therefore, mixed light of a broad emission spectrum can be generated. However, the thicknesses of the barrier layers and the quantum well layers are very thin (1 to 2 nm) in the LED chip. These thin barrier layers cannot confine the conductive carriers effectively, so the luminance efficiency is inferior. In addition, if the color of the mixed light generated by the LED chips differs from the predetermined color, it is hard to adjust the wavelengths and intensities of light generated by the quantum well layers, because the color and the color rendering index property of the mixed light are related to parameters (which are complex to analyze), such as compositions, energy bandgaps, as well as widths of the quantum well layers and of the barrier layers. Besides, in the quantum well and barrier layers of the LED chip, the luminance effect takes place.

Another light mixing LED chip is much easier, because the LED chip comprises only two or three active layers corresponding to different colors. Therefore, mixed light with predetermined wavelengths can be achieved by adjusting epitaxial parameters, such as the temperature, pressure, flowrate of ammonia, proportion of carrier gas, and/or doped magnesium or silicon.

Therefore, to generate a mixed white light the practical thickness of the barrier layer between two different color active layers has an order of around

hundred angstroms, i.e. the thickness of the barrier layer between the active layer sets can only be changed from 250 to 200 Å or from 250 to 300 Å, so that changing the thickness of the barrier layer can only fine-tune the color rendering coordinate in a narrow range of barrier layer thickness. As a result, if a mixed light of non-white light is required, the designer must consider three parameters at the same time, including pair numbers of the active layer sets, the thickness of the barrier layer, and the roughness degree of the quantum well layer. Too many parameters are too complex to control. In this case, it is useful to make a spectral fine-tune small current region on the chip, which is controlled by a microprocessor (Fig. 2).

Therefore, the designer must adjust at least two or three parameters to control the intensity ratio of different color lights. The chip can be rough-tuned first and then fine-tuned to achieve a color rendering coordinate. However, the method mentioned above is discontinuous and inaccurate, which is too complex and inefficient for a long lifetime.

In the light mixing LED, an undoped GaN layer can be inserted between the GaN buffer layer and the Si-doped GaN *n*-type contact layer and a Si-doped AlGaIn *n*-type cladding layer can be inserted between the Si-doped GaN *n*-type contact layer and the first GaN barrier layer (Fig. 2).

The first quantum well active layer is an active layer of green light with a peak wavelength close to 530 nm, and the second quantum well active layer is an active layer of blue light with a peak wavelength of about 460 nm. In case when the tunnelable barrier layer has a thickness of 14 nm, there is no obvious tunneling effect, and the light mixing LED emits only blue light. When the thickness of the tunnelable barrier layer is reduced to 10 nm, the tunneling effect of holes can just be observed. In spite of the mixed light emitted from the

light mixing LED, it is still dominated by blue light generated from the second quantum well active layer. However, the tunneling holes contribute a weak green light spectra, and result in the mixed light ranging on the chromaticity chart with a color rendering coordinate of  $X = 0.15, Y = 0.04$ , when the thickness of the tunnelable barrier layer is reduced to 7.2 nm, holes tunnel through the tunnelable barrier layer obviously, and the green light spectra appear clearly. In this case, the color rendering coordinate of the mixed light is located at  $X = 0.164, Y = 0.199$ . When the thickness of the tunnelable barrier layer is reduced to 6.0 nm, tunneling becomes more obvious, so that more holes in the quantum well of blue light tunnel through the tunnelable barrier layer to the quantum well of green light, causing the intensity of the green light to increase greatly. While the corresponding color rendering coordinate is located at  $X = 0.176, Y = 0.275$ . When the thickness of the tunnelable barrier layer is reduced to 4.5 nm, the intensity of green light is enhanced strongly and even higher than the intensity of blue light, and the corresponding color rendering coordinate is shifted to  $X = 0.189, Y = 0.445$ . When the thickness of the tunnelable barrier layer is further reduced to 3.6 nm, the corresponding color rendering coordinate is shifted to  $X = 0.210, Y = 0.623$ . The mixed light is much dominated by the green light. Finally, when the thickness of the tunnelable barrier layer is reduced to 2.5 nm, the majority of holes in the quantum well missing thickness of the tunnelable barrier layer is increased to 3.8 nm, the color rendering coordinate is shifted to  $X = 0.26, Y = 0.24$ , in the range of cold white light.

Another embodiment of light mixed LEDs provides three color lights for light mixing. The structure of the light mixed LED is basically similar to the previous light mixed LED, except for the inserting of one additional

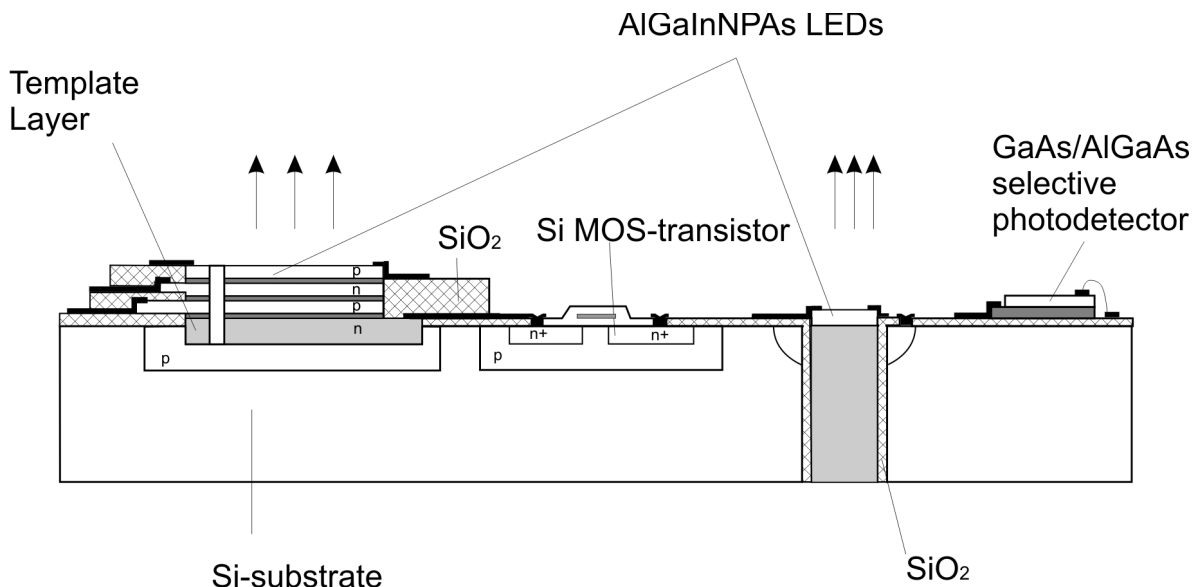


**Fig. 2.** Integrated RGB LED layers and MOS-transistor.

InGaN quantum well active layer of red light and one GaN tunnelable barrier layer between the first barrier layer and the first InGaN quantum well active layer. By adjusting the tunnelable barriers, the intensity ratio between the blue, green and red lights can be changed. As a result, the light mixing LED can emit any predetermined color of light.

By increasing the pair numbers of the quantum wells, it is possible to increase the luminance efficiency. A quantum well with a long wavelength can be achieved by increasing the In composition of the InGaN layer, or by incorporating *n*-type and/or *p*-type impurity, such as Si, Mg, Zn, etc., in the quantum well as a recombination center for holes and electrons.

Certainly, other quantum well active layers of different colors can be added, as long as the energy bandgap of an active layer adjacent to a *p*-type semiconductor side is larger than the energy bandgap of the active layer adjacent to the *n*-semiconductor side.

#### **4. Technology of nanostructures with a variable bandgap width**

One-chip white LED technology is based on varying the main composition of semiconductor compounds and their solid solutions in micro- and nanoregions. From a theoretical viewpoint, at certain thermodynamic conditions (volume, temperature, pressure, binding energy) all  $A^3B^5$  compounds form continuous rows of solid solutions [5]. However, among the practically realized technological parameters there are the regions of poor mutual solubility of  $A^3B^5$  compounds. Some solid solutions of mean compositions in the systems InGaAsP, InGaN, GaAsN and some others behave like that. In the work [5], offered to use are ionic technologies of expansion of solubility regions, which were widely used by us to prepare hard-solvable compositions of the multicomponent system InGaAsP [8, 11]. To integrate in one heterostructure active layers that radiate blue, green and red colors, it is possible by using a continuous row of solid solutions of III-nitrides and arsenides-phosphides [6]. Under ordinary temperatures and pressures, middle compositions of arsenides and nitrides – two based compounds of heteroelectronics – are dissolved badly. Interest to the three-component system of solid solutions of gallium arsenide-nitride is explained at least by three reasons.

First, they are a “bridge” between the system of solid solutions of nitride and arsenide phosphides – two basic compounds of multicomponent solid solutions, which in theory provide overlapping all the visible spectrum of radiation of LEDs and lasers, as well as selective sensitivity of photodetectors. However, the real mutual solubility of gallium arsenide and nitride in applied traditional technologies has considerable regions of insolubility for middle compositions [5]. Second, poor soluble compositions in nanoregions can create quantum dots of arsenides in the matrix of nitrides, what stimulate theoretical and experimental researches of mechanisms

and terms of their creation and stable existence. These mechanisms strongly differ from traditional approaches for massive crystals and microscopic epitaxial structures. Third, gallium arsenide and nitride find wide application in alarm-lighting and telecommunication technique due to unique parameters: LEDs and lasers are created on their basis for ultraviolet, visible and infra-red ranges of wavelengths; high electron mobility transistors (HEMT), operating at frequencies higher than 100 GHz on the power of ten watts, which provides operation at temperatures close to 400 °C; selective photodetectors with suppression of sensitivity to the sun radiation up to  $10^5$  times; physical and biological sensors.

In formation of nano-sized heterostructures based on binary compounds and their solid solutions, widely used are the methods of molecular-beam and MOC-hydride epitaxy. In these processes, necessary atomic compositions of solid solutions are set by fluxes of proper elements from III and V groups or molecules of their compounds, with thermal energies of the order of  $k_B T$ .

When growing  $A^3B^5$  heterostructures, the speed of growth is mainly determined by the speed of deposition on the substrate inherent to atoms of the third group elements. By changing this speed, it is possible to control the speed of growth by setting the proper program in wide limits from very low ( $\sim 1 \text{ \AA/s}$ ) to comparatively high ( $50 \text{ \AA/s}$ ). A low speed of growth is used if necessary to control the thicknesses and atomic composition of very small nanoregions, for example, quantum dots. When preparing the multicomponent solid solutions, it is required an extraordinarily complex setup and computer controlling program, which becomes yet more complicated by the kinetics of building-in for the fifth group atoms. Offered in this work is a new approach to nanoepitaxy of  $A^3B^5$  heterostructures, which consists of replacing only the atoms of the fifth group in a basic crystalline lattice that remains quasi-stable in the process of epitaxy.

In spite of large scientific and practical interest to the nanoepitaxial structures used in bandgap engineering aimed at solid solutions of gallium arsenide-nitrides and related compounds, the search for adequate epitaxy methods is weakly reflected in literature. Many authors, getting real heterogeneous structures, in the case of nanoregions use the model of insolubility valid for volume crystals. Such a position brakes development of nontraditional methods to obtain nano-heterostructures for practical applications.

In this work, we have tried to develop an alternative method for preparation of heterogeneous gallium arsenide-nitrides [12]. It consists of the substitution of part of arsenic atoms by the low-energy ions of nitrogen in the solid phase of gallium arsenide monocrystalline film. To increase the energy and mobility of the built-in elements, we offer to supply them by epitaxy from low-energy plasma with the ion energy of the order of several electronvolts. This is technologically comfortable and practically important

for the solid solution of gallium arsenide-nitrides grown on a gallium arsenide substrate to substitute a part of arsenic ions with the ionic radius 0.118 nm with nitrogen ions possessing the radius less than 0.071 nm.

The features of preparation of monocrystalline nanostructures from low-energy plasma is interesting, because these ions do not violate crystalline lattice structure, as in the case of implantation of impurities, and at the same time have a high mobility of volume migration, which provides “soft” substitution of atoms similar to the growth of monolayers from a liquid phase, catalytic action of which promotes high perfection and dislocation free micro- and nanostructures of gallium arsenide obtained by the vapour-liquid-solid mechanism. Deep understanding of the mechanisms of formation of GaAsN/GaAs heterostructures on a gallium arsenide substrate in low-energy nitrogen plasma opens a way for their controlled growth and determination of conditions providing not only oriented growth but also assembling the quantum points of arsenides to stimulate their self-organisation in the matrix. This opens a perspective of using nitrides for creation of new devices, such as, for example, quantum computers [13].

The conditions of condensation are determined by correlation between the speed of supplying the atoms and alteration of the surface layers. Preparation of heterostructures is related to formation of a new atomic layer with another element composition, as compared with that in the previous layer. Introduction of atoms or molecules with a certain concentration to beams of ions of the third and fifth groups of the periodic system allows to form complicated multicomponent structures with preset electronic and optical parameters. It is conditioned by point delivery of energy by ions into the surface and more deep monolayers of structures, which facilitates the kinetic processes of atomic migration at the comparatively low middle temperatures of substrate [5]. In its turn, lowering the temperature of epitaxy to 200-300 °C facilitates the requirements to sublattices of heterolayers and diminishes mechanical strains created during cooling the structures after epitaxy.

Controlling the composition of multicomponent  $A^3B^5$  solid solutions is possible by computer adjustment to obtain a smooth change of parameters in the growing layer lattice, in relation to the substrate, to get the necessary energy gap, electric and optical characteristics. As shown in [8], solid solutions with substitution of  $A^3$  and  $B^5$  have the features of solubility and growth of layers, which are determined by sizes of atoms and force of atomic bonds. When substituting  $A^3$  elements at comparatively low temperatures (about 300 °C) their adhesion coefficients are equal to unity, and the composition of solid solution is determined by the ratio of atomic fluxes. The same mechanism will be realized at epitaxy from the ionized flows.

In the course of epitaxial growth, there takes place minimization of the total free energy by an exchange of atoms in sublattices of the third and fifth groups in the

growing layer and monolayer that grows on it. This process is determined by overlapping the electronic clouds of neighboring atoms in crystal. The increase of temperature results in increase of the vapor pressure above the surface of solid solutions, which leads to distinction of losses at the surface and, consequently, to the difference in composition of layers with changing the ratio of falling fluxes.

It is known that the vapor pressure of  $A^3$  above  $A^3B^5$  compounds is close to that of flow above the pure element. With an increase in temperature, there is enriching the surface by more volatile elements of  $A^3$ . The substantial losses of In take place at growth temperatures higher than 560 °C, losses of Ga – at 650 °C, losses of Al – at still higher temperatures. In solid solutions with a substitution of atoms of the fifth group, there is no direct accordance between the built-in speed of components of the fifth group and the relative intensity of flows of these elements.

The mechanism of epitaxial growth becomes complicated by different mobility and lifetime of elements on surface. When growing the epitaxial layers from  $A^3B^5$  solid solutions, it is necessary to limit flow of more active components and to provide an excess of less active atoms and molecules. At the temperatures of desorption, into the place of desorbed molecules more easy molecules (nitrogen) are built-in and their concentration is increased.

When the flows are ionized, the built-in speed, mobility, lifetime, coefficients of adhesion, adsorption, desorption and segregation of components change substantially, which should be taken into account when computer controls the flow parameters. Thus, during ionization of flows in the processes of vapor or molecular-beam epitaxy of  $A^3B^5$  compounds and their multicomponent solid solutions, there are the following sub-processes that must be taken into account to prepare layers of the set element composition:

- 1) introduction of ions;
- 2) migration of ions and atoms along the surface and inside subsurface layer;
- 3) formation of binary, triple and more complex stable compounds of atoms on the surface;
- 4) decomposition of steady formations of atoms under action of the energy of the following ion;
- 5) replacement of elements  $A^3$  and  $B^5$  in surface sublattices, for example, arsenic in the lattice of GaAs by nitrogen.

The analysis of formation processes for the element composition GaAsN during epitaxial growth was made in the works [14, 15]. With increase of the growth temperature, there is an exchange between ions of arsenic and nitrogen, which results in strong lowering the concentration of nitrogen atoms  $n_N$ . It is explained by the thermally activated processes of segregation-desorption of nitric surface or nitric monolayer of crystalline lattice. Arsenic ions with the energy sufficient to pass the upper monolayers take place of the gone nitrogen atom. Mathematically, it may be shown

$$\frac{dn_N}{dt} = \gamma \Phi (1 - n_N) - \frac{n_N}{C_a}, \quad (1)$$

where  $\gamma$  is the activation coefficient,  $\Phi$  is the nitride ion flux,  $C_a$  is the thermal activation speed.

The term  $-\frac{n_N}{C_a}$  corresponds to the loss of nitrogen from the monolayer. It can be described kinetically through the constant of speed for thermal activation with the energy of  $E_a$ :

$$\frac{1}{C_a} = \frac{1}{C_{a0}} \exp\left(-\frac{E_a}{kT}\right), \quad (2)$$

where  $C_{a0}$  is the constant of the thermal activation speed.

It is commonly accepted that the main problem in growing the heteroepitaxial layers of  $A^3B^5$  is to provide accordance between parameters of crystalline lattices. Stringfellow binds to it the solubility of solid solutions, too [16]. However, here dynamics of atoms for both the third and fifth groups on a growing surface is not taken into account. At nitridization of GaAs substrates in atmosphere of neutral excited atoms of nitrogen for 10 min at the temperature 600 °C on a surface, the layer of gallium nitride appears with the thickness close to 1-2  $\mu\text{m}$ , thus, between it and GaAs, the layer of GaAsN with a variable composition appears. At lower temperatures 200 and 400 °C, there observed destruction of crystalline lattice by high-energy excited atoms of nitrogen – the process similar to ionic implantation of impurities, when the energies 100 to 300 keV are used. At the temperature 600 °C, one can observe annealing of the disordered phase of GaAsN, as a result of which GaN monocrystalline layer and graded bandgap layer of  $\text{GaAs}_x\text{N}_{1-x}$  appear (Fig. 3).

### 5. Nanotemplate $\text{Si}/\text{A}^3\text{B}^5$ integration technology

Combination of transistors on silicon with the heterostructures of  $\text{A}^3\text{B}^5$  is an actual problem in creation of integrated functional devices on one chip ( $\text{Si} / \text{A}^3\text{B}^5$ ). In spite of the fact that the first one-chip  $\text{Si} / \text{A}^3\text{B}^5$  devices were already offered by us in 1972 [17] and realized in 1975 [18], the search of new technologies proceeds actively. For the large diameters of silicon substrates, technology of nanotemplate  $\text{Al}_2\text{O}_3$  is interesting (Fig. 4) [19]. They chemically contact on the Si-surface, make initial growth surface of new epitaxial layers, predetermine diminishing the number of defects, by comparison to that of the initial surface (Fig. 5).

One of the attractive template is the self-organized anodized oxide of aluminum (TAOA). TAOAs that have sizes from sub-micrometer to nanometer cause large interest when forming electronic, optoelectronic and micro-mechanical nanodevices as well as creating single electron transistors capable to operate at room temperature.

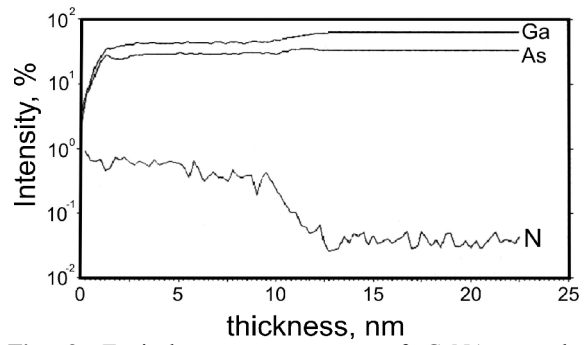


Fig. 3. Typical mass-spectrogram of GaNAs nanolayers prepared by nitric low energy plasma epitaxial growth.

There is an investigation of TAOA on Si-substrate and its parameters (radius and height) in the work [20]. Optimum template parameters provide dislocation-free relief of new epitaxial layers. At the large radius of nanoholes there exist asymptotic approaches to thin film decision. However, for small radii of nanoformations a picture differs from that of a two-dimensional thin film. It should be noted that even at large lattice mismatch (nearly 5 %), there are critical sizes for which acceptable dislocation-free layers exist.

In Fig. 2, one can see topology of one-chip white LED integrated with TAOA.

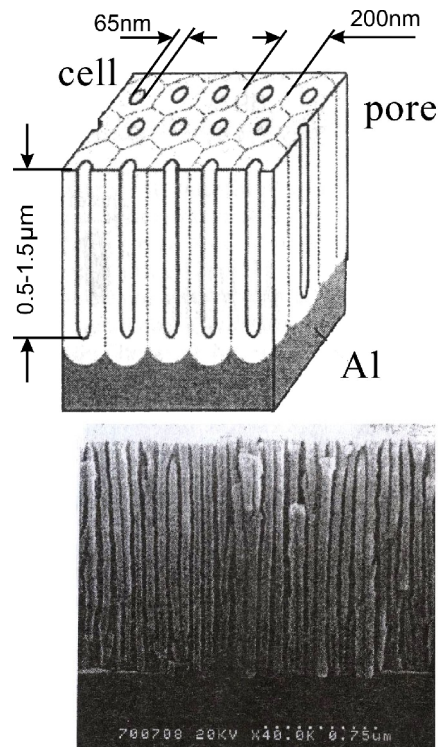
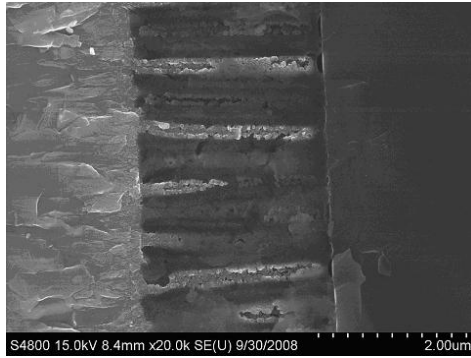


Fig. 4. (a) Schematic view of anodized aluminum oxide template; (b) anodized aluminum oxide template formed on 1.5  $\mu\text{m}$  Al layer that was evaporated using the magnetron facility on n-Si substrate of 100 mm diameter with the crystallographic orientation (100) and the sheet resistance 4  $\text{Ohm}/\square$ .





**Fig. 5.** Cross-section secondary-electron image of the GaN film grown on the Al anodic oxide prepared on (100) Si substrate.

## 6. Hybrid integration technology as a currently alternative

In this stage of integration technology development, acceptable are the hybrid integrated circuits for white light solid-state sources based on the structures  $\text{Si} / \text{A}^3\text{B}^5$ . Thus, it is necessary to take into account both electrical parameters of hybrid matrixes of superbright LEDs chips and geometrical location of them on the topology of matrix for the most optimum mixing of light flows. The hybrid integrated circuit consists of the following obligatory parts: LED chips – 3 matrixes of superbright RGB LEDs, microcontroller, commutator unit based on MOS transistors (Fig. 2). Hybrid IC serves as a model of monolithic IC and can be used in practice, when the cost is not important.

Application of a microcontroller in the control unit is caused by the necessity to keep radiation power at a constant level and to balance white light at a permanent level, regardless of temperature changes. Adjusting light emission of every chip is carried out using pulse current with pulse-width modulation (PWM). From the outputs, the PWM signal comes to commutators of MOS transistors. The middle current is set through the chips of matrix at the level of 350 mA. Initially, the PWM off-duty factor is nearly 50 %. In the process of natural degradation of matrixes, there observed lowering the brightness of LED luminescence, and the PWM off-duty factor increases up to 80-90 %.

Red chips are also the receivers of feedback signals that are used for measurements of radiation power for every chip. When measuring the radiation power of a dark blue LED, the red LED is used as a photodetector. Directly before measurements, the red LED is shunted by a resistor to accelerate transient processes. The next red LED is used for measuring the radiation power of green and first red chips. Farther, the feedback signal comes to 10-bit analog-digital input and is processed by the microcontroller program.

Being based on the obtained signal, the microcontroller corrects the PWM signal for every LED with the purpose to support the radiation power and

balance of white light at a set level regardless of changes in temperature and natural degradation of heterostructures.

The program of this microcontroller periodically carries out measurements of the intensity of light flows for each color, and on the basis of the data performs calculation of off-duty factors for PWM signals controlling the current of LEDs. Measurements of the light flow intensity are performed within a few microseconds, which remains unnoticeable for human sight. In the course of measurements, the LED of only one color is switched-on, while two others stay off. Thus, due to the control system, the brightness and balance of white light for the lamp stay at a permanent level. To solve the task of mixing these three colors, with the purpose to obtain homogeneous white light, a few methods of mixing were considered and the optimal one is selected in respect to overall, manufacturability and design aesthetics. As a light-mixing element, used was a retort of opal glass with a reflector. Color mixing takes place due to multiple reflections of light fluxes from the retort walls. To prevent mechanical damage, a polycarbonate retort with similar optical properties instead of glass can be used.

Our pilot sample of a white LED source is based on nine active LED chips for red, green and dark blue colors as the source of light, and a microcontroller as a control unit. The number of chips was chosen taking into account the total light flux equivalent to that of the 60 Watt incandescent lamp, and can be increased without considerable changes in the circuit.

The basic problem of structurally-technological association of powerful radiative elements in matrixes is effective heat sink and total candle-power radiation of a matrix [21]. To provide good heat sink from the active layers of heterostructures on a sapphire substrate, we used chips with removed substrate and contact system connected directly to  $n\text{-}n^+$  layers of the structure. For chips with the one-sided location of contact grounds and transparent sapphire substrate, used is flip-chip technology [22]. For matrixes, radiating a dense light flux (traffic-lights, lighting lamps), the chip component density is selected with account of heat dispersion in the base of matrix and overlapping the chip directional diagrams. From the thermal viewpoint, the packaging density for radiative chips is determined as

$$\alpha = P_m(T) / P_{\text{LED}} \cdot S \left( \text{elements} / \text{cm}^2 \right), \quad (3)$$

where  $P_m$  is the maximal power dispersed by the matrix at this temperature;  $P_{\text{LED}}$  is the middle dispersion power of one chip;  $S$  is the matrix area. The middle power of one chip heat dispersion is equal

$$P_{\text{LED}} = [1 - \eta(T)] P_e / N = [1 - \eta(T)] P_{e\text{LED}}, \quad (4)$$

where  $\eta(T)$  is the external quantum efficiency of a single chip at this temperature;  $P_e$  – electric power consumed by the matrix;  $N$  is the number of chips in the matrix;  $P_{e\text{LED}}$  – electric power consumed in one chip. The maximal possible chip packaging density in the matrix is equal

$$\alpha_T = P_m(T) / [1 - \eta(T)] P_{eLED} \cdot S. \quad (5)$$

It follows from (5) that attaining the increase in the packaging density is possible not only by the choice of heat-dissipative construction and lowering the chip electric power but also increasing the external quantum efficiency  $\eta$  with taking into account its temperature dependence. Thus, the maximal packaging density is reached when using close to zero or positive dependence of the external quantum efficiency on temperature [18] typical for LEDs based on III-nitrides.

On the other hand, the increase in the packaging density is required to provide a set total axial candle-power within the range of operation temperatures. As overlap of solid angles for chip directional diagrams takes place, the number of chips on unit area can be defined via the ratio of the aperture angle for the matrix  $\gamma_m$  to that for a single chip  $\gamma_c$ :  $\gamma = \gamma_m / \gamma_c$ .

Based on the performed analysis, the optimum packaging density for chips in the matrix should be

$$\lambda \leq \alpha \leq \alpha_T. \quad (6)$$

Light-emitting diodes based on AlInGaP have a stronger temperature dependence of radiation than those made of III-nitrides. Therefore, in the matrixes of LEDs based on AlInGaP the less packaging density can be realized as compared to that in III-nitrides LED matrixes. For functional chip integration on the basis of III-nitrides and AlInGaP in one integrated circuit (for example, RGB sources), the maximum degree of integration is determined by location of chips on AlInGaP. Overlap areas of matrixes for the examined two chip variants are presented in Fig. 6.

Overlapping the areas (shaded parts in the figure) is determined by the degree of integration in functional units containing chips on nitrides and aluminum, indium, gallium phosphides.

For Si/A<sup>3</sup>B<sup>5</sup> one chip integration it is necessary to make red-radiative layers from nitrides-arsenides or indium rich nitrides only (Fig. 1). Integral RGB LED structure heats Si-substrate that usually can dissipate no more than 5 W/cm<sup>2</sup>.

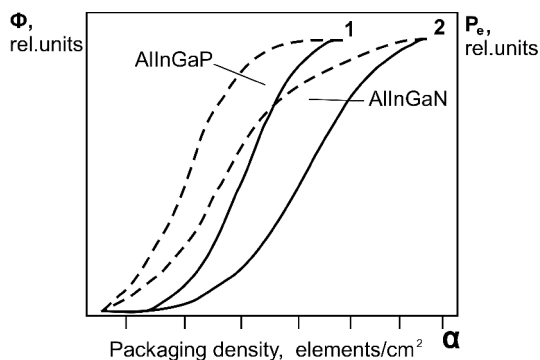


**Fig. 6.** Dependences of the total light intensity  $\Phi$  (dotted lines) and consumed power  $P_e$  (solid lines) for the elements based on AlInGaP (1) and AlInGaN (2).

Planning the choice of one or another construction and technology for matrixes of powerful light-emitting diodes, it is necessary, foremost, to optimize taking the heat from radiative areas. This choice is substantially facilitated when being based on understanding the thermal processes in chips, substrates, radiators and transitional layers applied in assembling. Research of these processes and their influence on optical properties of a matrix is important not only to develop technology but also can serve as an initial base for a potential consumer. In this case, the elements of matrix construction are transformed by the developer of signal-lighting device on the basis of LED matrixes into the structure of control units and construction of the optical system of hybrid optoelectronic devices. As shown in [21], the dynamic schemes for the controlling the power are optimum.

Constructions and technology of the powerful optoelectronic hybrid integrated circuits (POHIC) allow to integrate in a single technological cycle semiconductor radiative and receiving chips, microoptic, circuits of supply and control. However, the economic laws of production impose hard restraints on the choice of possible decisions. Cost of POHIC includes the cost of chips for powerful superbright LEDs, substrates, microoptics as well as the cost of work, assembling and control of POHIC. At the low integration level (2×2; 3×3; 5×5), the technological part of the total worth makes an insignificant fraction as compared to the cost of powerful chips. With increasing the integration degree, the cost of POHIC diminishes, until limitation of the possibility for heat-taking from the elements of matrix in this construction arises. Therefore, the improvement of heat-dissipation from chips is the actual task before wide application of powerful LED matrixes. Information perceived by the visual analyzer of man is determined not only by the brightness of emitter luminescence, as it is usually considered, but by the whole complex of radiation characteristics: amplitude, duration and frequency of excitation pulses, capability to interfere (by the degree of coherency) and the wavelength of light reflected from an object. I.e., the high brightness of luminescence is not the unique condition of good resolution of image but depends also on the background luminosity and contrast. With increase of the pulse current amplitude, realized in powerful LEDs is the mode of superluminescence, at which partial coherency of radiation becomes possible, which arises at less currents, when the temperature of chip active regions is lower. The common increase of light fluxes from the elements of matrix is achieved by application of the external reflectors integrated with substrate as well as microoptics.

## 7. Conclusions

We have realized monolithic and hybrid integration of RGB LED structures for mixing light to create white color and control its parameters by Si IC processor, integrated with LED structures in a single chip. It is

ascertained that many technological parameters that should be controlled during LED structure production and changing parameters of light with time and temperature can be stabilized by Si transistor IC driver, integrated with LED  $A^3B^5$  structures. The selective and lateral ion epitaxy of nanostructures in template technology corresponds to  $Si/A^3B^5$  integration of one chip white LED sources.

Optimal light mixing of integrated  $Si/A^3B^5$  one chip white LED depends on thermal conductivity of substrate and energetic efficiency of RGB radiative layers. The experimental technological investigation of hybrid packaged LED RGB chip integration, presented in this work, shows the way of monolithic integration that gives better parameters and low cost of white LED sources for lighting.

#### References

1. V. Osinsky, Information conception of image perception at solid state lighting // *Semiconductor Physics, Quantum Electronics & Optoelectronics* **10**, No. 3, p. 30-43 (2007).
2. V. Osinsky, P. Oleksenko, A. Palagin, et al., The problems of integration of heteroelectronic structures with silicon integrated circuits // *Tekhnologiya and konstruirovaniye v elektronnoi apparature* No. 1, p. 3-17 (1999) (in Russian).
3. V. Osinsky, V. Verbitsky, Yu. Mokeev et al., White superluminescent LED and the method of its production // *Patent of Ukraine #56544A*, 17.07.2002.
4. V.I. Osinsky, Cosmic nanotechnologies for creation of heterogeneous information environment. Technologies for creation of promising computer technique and systems with using the latest electronic base // *Collected papers of Institute of Cybernetics*, NAS of Ukraine, Kiev, 2000, p. 122-128.
5. V. Osinsky, V. Verbitsky, Band gap engineering: ion realisation of virtual quantum nanoelectronic heterostructures // *Optyko-elektronni informatsiino-energetychni tekhnologii* No. 1, p. 169-183 (2001) (in Russian).
6. V.I. Osinsky, Optoelectronic properties of heterogeneous semiconductors at superhigh time and space frequencies // *Proc. 5-th Intern. Symposium on Recent Advances in Microwave Technology*, Part II, Kiev, September 11-16, 1995, p. 433-436.
7. V.I. Osinsky, Super high-speed optoelectronics: technological fundamentals and economics // *Proc. SPIE. Optoelectronic Information Technologies* **4425**, p. 263-271 (2000).
8. V. Osinsky, F. Katsapov, V. Privalov, Integrated LED structures obtained by gas charge epitaxy of  $GaAs_{1-x}P_x$  films // *Proc. Belorussian Academy of Sciences*, Phys.-math. series No. 5, p. 73-76 (1977).
9. V. Osinsky, F. Katsapov, E. Tyavlovskaya, Structural perfection of selective GaAs LED regions in Si substrate windows // *Phys. status solidi (a)* **82**, No. 2, p. 174-179 (1984).
10. Chen On, Chen-Ke Hsu, Light Mixing LED. *US Patent No. 0006375A1*, 2006.
11. V. Osinsky, F. Katsapov, E. Tyavlovskaya, The method of semiconductor structure production. *Patent of USSR N 1245159A*, 1984.
12. D. Mazunov, V. Osinsky, V. Verbitsky, V. Glotov, GaAs nitridization in low energy plazma // *Proc. 6-th All-Russian Conference "Nitrides of gallium, indium and aluminum structures and devices"*, St.-Petersburg, June 18-20, 2008, p. 48.
13. A. Palagin, V. Osinsky, V. Verbitsky et al., Quantum Processor // *Patent of Ukraine No. 57825*, 2000.
14. Z.Z. Bandic, R.J. Hauenstein, M.L. O'Steen, T.C. McGill, Kinetic modeling of microscopic processes during electron cyclotron resonance microwave plasma-assisted molecular beam epitaxial growth of GaN/GaAs-based heterostructures // *Appl. Phys. Lett.* **68**(11), p. 1510-1512 (1996).
15. V. Verbitsky, S. Osinsky, A. Sarikov, Calculation of elemental composition for graded bandgap  $A^3B^5$  structures for white LEDs // *Fizicheskaya inzheneriya poverkhnosti* **1**, No. 3-4, p. 341-346 (2003) (in Russian).
16. G.B. Stringfellow, Miscibility gaps in quaternary III-V alloys // *J. Crystal Growth* **58**, p. 194-202 (1982).
17. V. Osinsky, N. Kostiukevich, Integral Optron // *Patent of USSR No. 551730*, 1973.
18. V. Osinsky, *Integrated Optoelectronics*. Nauka i tekhnika, Minsk, 1977, p. 248 (in Russian).
19. V. Osinsky, V. Labunov, G. Gorokh, N.M. Liahova, N.O. Liahova, D. Solovey, Template layers for  $Si/A^3B^5$  nanostructures // *Elektronika i svyaz', temat. vypusk "Problemy elektroniki"* No. 1-2, p. 70-75 (2008) (in Russian).
20. V. Osinsky, I. Poliakov, G. Gorokh, N. Liahova, S.J. Pearton et al., Non-polar GaN prepared on Si substrates by hydride vapor phase epitaxy using anodized Al nanomask (to be published in *Appl. Phys. Lett.*, 2009).
21. V. Osinsky, V. Zavalishin, A. Radkevich, D. Murchenko, I. Tuchinsky, Yu. Trocenko, V. Grunianska, Diode source for common lighting made by hybrid integration of  $A^3B^5$  RGB chips with Si transistor structures // *Elektronika i svyaz', temat. vypusk "Problemy elektroniki"* No. 1-2, p. 84-89 (2008) (in Russian).
22. V. Osinsky, I. Tuchinsky, V. Zhora, V. Grunianska, N. Liakhova, A. Rubanchuk, Flip-chip LED packing technology used flexible carriers on polyimide base // *Elektronika i svyaz', temat. vypusk "Problemy elektroniki"* No. 2, p. 5-8 (2006) (in Russian).